Bioactive Materials 32 (2024) 292–303

Contents lists available at ScienceDirect

Bioactive Materials

journal homepage: www.keaipublishing.com/en/journals/bioactive-materials

Extracellular matrix-templating fibrous hydrogels promote ovarian tissue remodeling and oocyte growth

Claire E. Nason-Tomaszewski [a], Emily E. Thomas [a], Daniel L. Matera [b], Brendon M. Baker [a], Ariella Shikanov [a,c,d,*]

[a] Department of Biomedical Engineering, University of Michigan, Ann Arbor, MI 48109, USA
[b] Department of Chemical Engineering, University of Michigan, Ann Arbor, MI 48109, USA
[c] Department of Obstetrics and Gynecology, University of Michigan, Ann Arbor, MI 48109, USA
[d] Cellular and Molecular Biology Program, University of Michigan, Ann Arbor, MI 48109, USA

ARTICLE INFO

Keywords:
Biomimetic matrix
Ovarian follicle
Fibrous hydrogels

ABSTRACT

Synthetic matrices which mimic the extracellular composition of native tissue create a comprehensive model for studying development and disease. Here, we have engineered a composite material which retains cell-secreted ECM for the culture of ovarian follicles by embedding electrospun dextran fibers functionalized with basement membrane binder (BMB) peptide in PEG hydrogels. In the presence of ECM-sequestering fibers, encapsulated immature primordial follicles and ovarian stromal cells aggregated into large organoid-like structures with dense deposition of laminin, perlecan, and collagen I, leading to steroidogenesis and significantly greater rates of oocyte survival and growth. We determined that cell aggregation restored key cell-cell interactions critical for oocyte survival, whereas oocyte growth was dependent on cell-matrix interactions achieved in the presence of BMB. Here we have shown that sequestration and retention of cell-secreted ECM along synthetic fibers mimics fibrous ECM structure and restores the cell-cell and cell-matrix interactions critical for engineering an artificial ovary.

1. Introduction

In vitro systems are valuable tools for regenerative medicine and models to study biological mechanisms in a controlled environment. Within the native tissues, ECM plays an important biological role, promoting reciprocal cell-matrix interactions through integrin binding and other receptors, supporting expansion and proliferation through matrix remodeling, and modulating the release and sequestration of matrix-bound growth factors [1,2]. Existing hydrogel-based 3D culture systems support co-culture of multiple cell types and organoid-like structures and recapitulate the bidirectional exchange of soluble cytokines mimicking to some extent the physical and biochemical microenvironment of the extracellular matrix (ECM) in which cells reside *in vivo* [3,4]. However, as the field of regenerative medicine and tissue engineering progresses, there is a growing need for biomimetic *in vitro* systems that promote reciprocal cell-matrix interactions and may help elucidate how these interactions drive the behavior of cells, cell clusters and organoid-like structures *in vitro*.

Ovarian follicles are the multicellular aggregates in the ovary responsible for a woman's fertility and ovarian endocrine function. Currently, young women and prepubertal girls diagnosed with cancer and facing ovo-toxic treatments have limited options to preserve their fertility, with cryopreservation of ovarian tissue prior to chemotherapy being the most promising route [5,6]. However, only primordial and early-stage primary follicles survive cryopreservation. Ovarian follicles share many similarities with tissue organoids including a diverse composition of cells, three dimensionality, cell proliferation and differentiation. Follicles are complex multi-cellular structures each containing an oocyte (egg) surrounded by hormone-producing somatic cells. Periodically, a small cohort of primordial follicles activates and initiates the growing process, called folliculogenesis, culminating with ovulation [7–9]. The survival and growth of follicles in the early stages is dependent on paracrine signaling from surrounding follicles [10–13] and stromal cells [14–16], as well as physical cues from the ECM [17–19]. As follicles grow, they degrade and soften the surrounding ECM and deposit new matrix to accommodate volumetric expansion in

Peer review under responsibility of KeAi Communications Co., Ltd.
* Corresponding authorDepartment of Biomedical Engineering, University of Michigan, Ann Arbor, MI 48109, USA.
E-mail address: shikanov@umich.edu (A. Shikanov).

https://doi.org/10.1016/j.bioactmat.2023.10.001
Received 16 March 2023; Received in revised form 14 August 2023; Accepted 1 October 2023

later stages [20,21]. Softening of the matrix can be readily mimicked *in vitro* with degradable hydrogels which provide a stiff-to-soft transition necessary for follicle growth, but the reciprocal remodeling of ECM, crucial for cell-matrix interactions, remains a challenge to incorporate in *in vitro* settings [22–26]. We recently engineered reciprocal cell-matrix interactions by functionalizing degradable PEG hydrogels with ECM-sequestering peptides which retained cell-secreted ECM within the hydrogel, improving growth and maturation rates of secondary follicles [17], but the structure of the newly deposited ECM proteins was amorphous and did not mimic the highly fibrillar and dense ECM in which earlier stage primordial follicles reside [27,28]. Furthermore, a recently published study suggests that the complex fibrillar structure of perifollicular ECM supports physiologic follicle-matrix signaling *in vivo*, providing a critical design criterion for next-generation follicle culture [29]. To address this limitation, degradable synthetic hydrogels have been paired with tunable electrospun fibers which can be functionalized with bioactive ligands through Michael-type addition chemistry [30,31]. As such, we posit that sequestration and proper structural templating of cell-secreted ECM is crucial for the organization and controlled expansion of ovarian follicles.

To match the multicomponent composition of the native extrafollicular tissue environment, here we describe a novel approach to creating structurally and biologically relevant matrix in the form of 3D fiber-reinforced hydrogel composites that can template cell-secreted ECM along the fibers. These hydrogels offer independent control over both the bulk material (PEG hydrogel crosslinked with proteolytically degradable peptides) and fiber constituents (electrospun dextran fiber segments decorated with bioactive peptides). The bulk hydrogel and the fiber components were modified with ECM-binding peptides to sequester cell-secreted ECM molecules to allow encapsulated follicles to reconstruct the extrafollicular matrix compositionally and structurally similar to native tissue. We utilized this novel composite hydrogel system to culture the most immature primordial follicles and demonstrated markedly improved oocyte survival in a matrix that combines follicles, stromal cells, and ECM for mimicking the ovarian microenvironment. This work highlights a distinction between unguided ECM deposition within a bulk hydrogel in contrast to the creation of fibrous tissue-like ECM templated by synthetic fibers which we find (1) drives the organization of the follicle-like structures with oocytes surrounded by somatic cells, and (2) promotes follicle survival, growth, and hormone production. Moreover, the design of this matrix and the ability to sequester cell-secreted ECM likely holds utility for a wider range of tissue engineering applications.

2. Materials and methods

2.1. Fiber fabrication and functionalization

All reagents were purchased from Thermo Fisher unless specified otherwise and all peptides were purchased from GenScript (Piscataway, NJ, USA). Dextran vinyl sulfone (DexVS) was synthesized using a previously established protocol for vinyl sulfonating polysaccharides adapted for use with high MW dextran (MW 86 kDa, MP Biomedicals, Santa Ana, CA) [16,25,26]. Briefly, pure divinyl sulfone (12.5 mL, Fisher Scientific, Hampton, NH) was added to a sodium hydroxide solution (0.1 M, 250 mL) containing dextran (5 g). This reaction was carried out at 1500 RPM for 3.5 min, after which the reaction was terminated by adjusting the pH to 5.0 via the addition of hydrochloric acid. All reaction products were dialyzed for 5 days against Milli-Q ultrapure water, with two water exchanges daily, and then lyophilized for 3 days to obtain the pure product. Functionalization of DexVS was characterized by 1H-NMR spectroscopy in D_2O and was calculated as the ratio of the proton integral (6.91 ppm) and the anomeric proton of the glucopyranosyl ring (5.166 and 4.923 ppm); here a vinyl sulfone/dextran repeat unit ratio of 0.376 was determined for DexVS polymers.

For electrospinning, DexVS was dissolved at 0.6 g mL^{-1} in a 1:1 mixture of Milli-Q ultrapure water and dimethylformamide with 0.015% Irgacure 2959 photoinitiator. Methacrylated rhodamine (0.5 mM; Polysciences, Inc., Warrington, PA) was incorporated into the electrospinning solution to fluorescently visualize fibers. This polymer solution was utilized for electrospinning within an environment-controlled glovebox held at 21 °C and 30% relative humidity. Electrospinning was performed at a flow rate of 0.3 mL h^{-1}, gap distance of 5 cm, and voltage of - 10.0 kV onto a grounded collecting surface attached to a linear actuator. Fiber layers were collected on glass slabs and primary crosslinked under ultraviolet light (100 mW cm^{-2}) and then secondary crosslinked (100 mW cm^{-2}) in a 1 mg mL^{-1} Irgacure 2959 solution. After polymerization, fiber segments were resuspended in a known volume of PBS (typically 3 mL). The total volume of fibers was then calculated via a conservation of volume equation: total resulting solution volume = volume of fibers + volume of PBS (3 mL). After calculating total fiber volume, solutions were re-centrifuged, supernatant was removed, and fiber pellets were resuspended to create a 1.1 vol% fiber solution, which were then aliquoted and stored at 4 °C. To support ECM deposition, 2.0 mM BMB peptide (GCREISAFLGIPFAEPPMGPRRFLPPEPKKP, GenScript), was coupled to vinyl sulfone groups along the DexVS backbone via Michael-type addition chemistry for 30 min. Fibers were loosely pelleted at 2000×*g* for 10 s then resuspended in hydrogel precursors for encapsulation with follicles and cells.

2.2. Hydrogel and peptide formulations

All hydrogels were formed using 8-arm PEG-vinyl sulfone (PEG-VS) (40 kDa, >99% purity, JenKem Technology) crosslinked via Michael-type addition with trifunctional (3 cysteine) plasmin-sensitive crosslinkers: a fast-degrading GCYKNRGCYKNRCG (YKNR), slow-degrading GCYKNSGCYKNSCG (YKNS), or non-degrading $GCYK_DNS_DG$-CYK_DNS_DCG (D-YKNS or YK_DNS_D) which incorporates the non-native D-isomers of lysine and serine to render the peptide nondegradable by plasmin. A 1:1 M ratio of YKNS (slow degrading) and YKNR (fast degrading) was used unless noted otherwise as this ratio has previously been shown to support folliculogenesis [17]. Before crosslinking, PEG was modified with basement membrane binding peptide (BMB bulk) or cysteines to serve as a non-sequestering control. Hydrogels had a final formulation of 5 wt% PEG, 0.75 mM bulk modification, and 3.08 mM total crosslinker resulting in a 1:1 stoichiometric ratio of -VS to thiol (-SH) groups. PEG and ECM-binding peptide were dissolved in isotonic 50 mM HEPES buffer (pH = 7.4 at 37 °C), mixed, and allowed to react for 15 min at 25 °C. Peptide crosslinkers were then dissolved in 50 mM HEPES and mixed with BMB-functionalized PEG. Complete hydrogel precursor solution was used to resuspend follicle and fiber pellets, and 5 μL drops were pipetted onto parafilm-coated glass slides. Hydrogels were crosslinked at 37 °C for 5 min then transferred to follicle maintenance medium (minimal essential medium Eagle-alpha modification [αMEM] supplemented with 1% (v/v) fetal bovine serum and 0.5% (v/v) penicillin-streptomycin) to terminate gelation.

2.3. Fiber and hydrogel characterization

Fiber lengths and widths in 10× images of suspended fibers were measured using ImageJ. Cysteine-modified bulk hydrogels with (n = 6) and without (n = 6) BMB-functionalized fibers were characterized through axial compression testing. To test the effect of cell-driven proteolytic degradation on hydrogels' mechanical properties, we embedded BMB-functionalized fibers and encapsulated stromal cells and follicles at a density of 0.4 ovaries/gel in bulk hydrogels modified with 0.75 mM BMB. These gels were characterized through axial compression testing on days 0 (n = 5) and after 18 days of culture (n = 6). Unconfined compression of 8 mm diameter cylindrical hydrogel samples was performed on a TA HR 30 Discovery Hybrid Rheometer with an 8 mm parallel plate. Compression was performed at a rate of 5 μm/s until 40%

strain at 37 °C. Stress was calculated by division of force by cross-sectional area of the hydrogel sample, and the elastic modulus was found by calculating the slope of the linear elastic region of the resulting stress-strain curves. The mass equilibrium swelling ratio (Q_m) was calculated as the swollen hydrogel mass divided by the lyophilized hydrogel mass. Hydrogels were swollen overnight in phosphate buffered saline, weighed, then lyophilized until dry.

2.4. Follicle isolation, encapsulation, and culture

All animal procedures were performed in compliance with the Guidelines for the Care and Use of Animals at the University of Michigan. Procedures were approved by the Institutional Animal Care and Use Committee (IACUC) at the University of Michigan (PRO00009635). Female C57Bl/6 and male CBA mice were purchased from Envigo for breeding. Primordial follicles and stromal cells were enzymatically isolated from the ovaries of 5-day old B6CBAF1 pups to yield hundreds of follicles and cells for encapsulation. Ovaries were placed in warm Leibovitz's L-15 medium supplemented with 0.5% (v/v) penicillin-streptomycin and 2.5 mg mL^{-1} collagenase 1A (Sigma Aldrich) for 15 min, then transferred to fresh L-15 with PenStrep and vigorously pipetted for 3 min to remove the outermost follicles and cells, followed by enzyme quenching with fetal bovine serum (1% v/v). The remaining pieces of tissue were returned to the digestion medium for 15 min, followed by the dissociation and quenching steps. Follicles and cells were passed through a 40 μm cell strainer to remove larger follicles and pieces of undigested tissue, however the diversity and proportions of the remaining cells and follicles was assumed to resemble the native ovary. The follicle and cell suspension was pelleted at 100×*g* for 5 min. The supernatant was removed, and the pellet was resuspended with hydrogel precursors, then 5 μL droplets were pipetted onto parafilm-coated glass slides for gelation. Gels were transferred to pre-equilibrated follicle maintenance medium (minimal essential medium Eagle-alpha modification [αMEM] supplemented with 1% (v/v) fetal bovine serum and 0.5% (v/v) penicillin-streptomycin) and stored in an incubator (37 °C, 5% CO_2) for 30 min to 1 h. Follicles were cultured in 150 μL of follicle growth medium (αMEM supplemented with 1 mg mL-1 bovine fetuin (Sigma Aldrich), 3 mg mL-1 bovine serum albumin, 5 μg mL-1 each insulin-transferrin-selenium (Sigma Aldrich), and 10 mIU mL-1 recombinant human FSH (Gonal-F)) in individual wells of a 96-well plate for 18 days. Every two days, half of the growth medium was replaced with fresh growth medium. For experiments in which matrix metalloproteinases were inhibited, follicle growth medium was supplemented with marimastat (Sigma Aldrich) at 0.5 μM. Unless otherwise stated, 10 gels per condition were cultured for each experiment.

2.5. Follicle density, survival and activation

Initial follicle densities and subsequent activation and survival were quantified through immunofluorescent staining for FOXO3a, an oocyte activation marker which exports from the nucleus to the cytoplasm when activated (Supplemental Fig. 1). Hydrogels containing follicles were fixed for 1 h in 4% paraformaldehyde at room temperature then washed in PBS (3×, 15 min each). Samples were transferred to a 25% w/v solution of Optimal Cutting Temperature (OCT) medium in water for 24 h at 4 °C, followed by 24 h each in 50% OCT solution then 100% OCT at 4 °C. Samples were cryosectioned on a Microm HM 525 cryostat at −21 °C to make 200 μm thick sections. Samples were blocked for 12 h at 4 °C in 5% normal goat serum in PBS. Primary antibodies for FOXO3a (Cell Signaling Technology, 2497S) were diluted 1:250 in blocking solution and incubated for 12 h at 4 °C. Samples were washed in blocking solution (3×, 1 h each) then incubated with Hoechst 33342 nuclear stain (Thermo Fisher) and secondary antibodies (Thermo Fisher, AlexaFluor 647 A-21244) diluted 1:500 in blocking solution for 12 h at 4 °C. Samples were washed in PBS (3×, 1 h each) then mounted in concave slides with Prolong Diamond (Thermo Fisher). Tile scan z-stack images were captured on a Leica SP8 laser scanning confocal microscope to obtain full images of the entire cryosectioned sample.

Follicle activation was quantified from hydrogels cultured for two days to allow sufficient time for activation and to obtain accurate counts of healthy follicles which survived the dissociation and encapsulation process. Dormant and activated oocytes were manually counted from stained cryosections, in which activated oocytes exhibited distinct cytoplasmic staining of FOXO3a (Supplemental Fig. 1), and dormant oocytes were identified by the presence of a comparatively large cell (>10 μm) surrounded by at least two squamous cells with flattened nuclei visualized with Hoechst. Follicle activation after 2 days of culture was calculated by dividing the number of oocytes with cytoplasmic FOXO3a staining by the total sum of oocytes counted within each cryosection.

Encapsulated follicle densities at the start of culture and follicle survival after 18 days of culture were based on follicle densities within cryosections. Oocytes were identified based on size and visual appearance or FOXO3a staining. Denuded oocytes which appeared healthy (clear and round) were included in density calculations for their potential to be rescued and enveloped in cell aggregates. The volume of the cryosection was calculated from the cross-sectional area, measured in ImageJ, and the height of the z-stack image. This volume was then used to calculate the density of follicles (oocytes/μL) as presented in Supplemental Fig. 1, and an average density across multiple cryosections was extrapolated to the entire 5 μL gel for determining the approximate number of encapsulated follicles at the start of culture. Follicle densities after 18 days of culture were similarly determined from multiple cryosections, and this density was used to determine the approximate number of remaining oocytes in the entire hydrogel. Follicle survival was then calculated by dividing this approximate number of oocytes by the calculated average number of starting follicles in the hydrogel determined from samples after 2 days of culture.

2.6. Oocyte collection and in vitro maturation (IVM)

After 18 days of culture, hydrogels (n = 3 or 4) were proteolytically dissolved to release the encapsulated follicles and cells to assess maturation. Culture medium was removed from the hydrogels and replaced with equilibrated αMEM supplemented with 1.14 U mL^{-1} plasmin (Sigma Aldrich) and 2.6 Wünsch units mL^{-1} Liberase DH (Sigma Aldrich). Hydrogels were dissolved for 45 min at 37 °C in 5% CO_2 and pipetted every 15 min to aid in degradation. Follicles and cells were left to settle for 5 min, then the degradation medium was removed and replaced with 150 μL of equilibrated maturation medium (αMEM supplemented with 10% fetal bovine serum, 5 ng/mL epidermal growth factor, 1.5 IU mL^{-1} human chorionic gonadotropin, and 10 mIU mL^{-1} follicle stimulating hormone) for 20 h. Follicles were then treated with 0.03% hyaluronidase (type IV-S from bovine testes, Sigma Aldrich, 750–3000 IU/mg) to release cumulus oocyte complexes. Cumulus cells were removed, and oocytes were evaluated to determine meiotic stage and diameters measured in ImageJ. Oocytes which were fragmented, dark in appearance, or showing signs of degeneration were not included in counts of viable oocytes.

2.7. Immunostaining and confocal microscopy

Hydrogels containing follicles (n = 2) were fixed for 1 h in 4% paraformaldehyde at room temperature then washed in PBS (3×, 15 min each). Samples were transferred to a 25% w/v solution of Optimal Cutting Temperature (OCT) medium in water for 24 h at 4 °C, followed by 24 h each in 50% OCT solution then 100% OCT at 4 °C. Samples were cryosectioned on a Microm HM 525 cryostat at −21 °C to make 200 μm thick sections. Samples were blocked for 12 h at 4 °C in 5% normal goat serum in PBS. Primary antibodies for laminin (Abcam, ab80580), collagen I (Sigma Aldrich, SAB4500362), and perlecan (Santa Cruz Biotechnology, sc-33707) were diluted 1:250 in blocking solution and

incubated for 12 h at 4 °C. Samples were washed in blocking solution (3×, 1 h each) then incubated with Hoechst 33342 nuclear stain (Thermo Fisher) and secondary antibodies (Thermo Fisher, AlexaFluor 647, A-21247 and A-21244) diluted 1:500 in blocking solution for 12 h at 4 °C. Samples were washed in PBS (3×, 1 h each) then mounted in concave slides with Prolong Diamond (Thermo Fisher). Images were captured on a Leica SP8 laser scanning confocal microscope. All confocal images were captured using the same laser power, gain, and imaging parameters outlined in Supplemental Table 1. All confocal images are presented as maximum intensity projections of 200 μm thick hydrogel sections. A baseline subtraction was performed on all follicle images based on the mean intensity in order to reduce noise caused by autofluorescence. Mean fluorescence intensity measurements were taken from unaltered images in Leica LASX software. Fluorescence was measured from two cryosections per condition by randomly sampling 200 × 200 pixel (113.6 × 113.6 μm) regions across the cryosections. The average intensity of the region of interest was measured for each channel in the region of interest, then ECM fluorescence intensity was normalized to the nuclei (Hoechst) intensity of the same region to accommodate for loss of intensity and resolution of both ECM and nuclei fluorescence intensity as more light is scattered deep within samples. Each region of interest was treated as an individual sample for statistical analysis.

2.8. Hormone analysis

Follicle-secreted sex hormones androstenedione, estradiol, and progesterone were analyzed from the culture medium of encapsulated follicles and cells from days 10–18 of culture. Hormone analysis for varying follicle densities was performed on pooled medium from two gels and divided into three technical replicates. Hormone analysis for BMB bulk/BMB fiber gels and corresponding non-sequestering controls was performed on medium from individual samples for four biological replicates. Replicates of each condition were analyzed by the University of Virginia Center for Research in Reproduction Ligand Assay and Analysis Core (Eunice Kennedy Shriver NICHD/NIH Grant R24HD102061).

2.9. Statistical methods

Statistical analysis of follicle measures and ECM quantification was performed in GraphPad Prism 9. Follicle densities and activation after two days of culture were compared using an ordinary one-way ANOVA followed by a Tukey test to correct for multiple comparisons. Oocyte counts on day 18, oocyte diameters, average aggregate cross-sectional areas, and ECM mean fluorescence intensity were compared using Brown-Forsythe and Welch's ANOVA followed by a Tukey test to correct for multiple comparisons. Unless stated otherwise, data is presented as average ± standard deviation. $P < 0.05$ was considered statistically significant, and significance was defined as *$p < 0.05$, **$p < 0.01$, ***$p < 0.005$, ****$p < 0.0001$.

3. Results

3.1. Degradable PEG hydrogels support activation and co-culture of ovaries dissociated into individual primordial follicles and cells

Ovaries dissociated into individual follicles and cells were encapsulated in non-sequestering PEG hydrogels (n = 3 for each concentration) at concentrations ranging 0.2–1.0 ovary/gel to determine the extent of follicle activation and density sufficient for paracrine support without overwhelming the culture medium (Supplemental Fig. 1). Across all conditions, follicles exhibited similar rates of activation (~75%) after two days in culture, confirmed by the export of FOXO3a to the cytoplasm. Follicle survival across all conditions was approximately 10–20% with 0.2 ovary/gel exhibiting the lowest survival and 1.0 ovary/gel exhibiting the highest survival. At the lowest encapsulation density (0.2 ovary/gel) insufficient paracrine support likely led to follicle death, and at higher encapsulation densities (0.8 and 1.0 ovary/gel), the culture medium was quickly exhausted and did not support folliculogenesis as evidenced by dense cell clusters, shriveled degenerated oocytes, and acidic culture medium. Encapsulation of 0.4 ovary in a 5 μL gel was determined to be the optimal density for culture with 124 ± 23 follicles/μL, 4.18E6 ± 1.1E6 stromal cells/mL, and 77.8% ± 3.0% activation (Supplemental Fig. 1). To assess degradation the bulk elastic modulus was measured on days 0 and 18 showing that hydrogels soften from about 13.6 kPa with 95% CI [9.6 kPa, 16.1 kPa] to 1.9 kPa with 95% CI [1.5 kPa, 2.7 kPa] during culture (Supplemental Fig. 2).

3.2. Clustering of ECM-binding peptides on fibers increased ECM deposition

Modification of bulk PEG hydrogel with BMB peptide previously improved maturation rates of oocytes from larger more mature follicles [17]. Here we sought to determine whether the presence of fibers or BMB peptide would promote reclustering and ECM deposition after ovary dissociation and improve oocyte survival and growth. We first confirmed that the presence of fibers within the hydrogel did not affect the bulk mechanical properties of the gel (Supplemental Fig. 2). DexVS fibers measured an average 67 ± 67 μm in length and 2.1 ± 0.7 μm in diameter, which falls within the range of diameters of ovarian ECM fibers and bundles [29]. There was no statistical difference in elastic modulus or swelling ratio between hydrogels with and without embedded BMB-functionalized fibers at 2% v/v. Bulk hydrogels without embedded fibers have a median elastic modulus of 19.86 kPa with 95% CI [17.7, 22.6] and a swelling ratio of 24.8 ± 1.2. Hydrogels embedded with DexVS fibers have a median elastic modulus of 18.16 kPa with 95% CI [16.3, 20] and a swelling ratio of 23.9 ± 1.6. We cultured follicles in non-sequestering bulk hydrogels embedded with non-sequestering fibers ('Control Fibers'), bulk BMB-modified hydrogels without fibers ('BMB Bulk'), or non-sequestering bulk hydrogels embedded with BMB-functionalized fibers ('BMB Fibers') (Fig. 1a). As expected, in the control fiber condition, follicles and cells did not bind to fibers, and remained in small separated, clusters. Insufficient cell proliferation, required for hormone production and signaling, and minimal aggregation around oocytes, critical for oocyte growth, contributed to low oocyte survival and growth with only 2% oocytes per gel surviving to day 18 and an average oocyte diameter of 36 μm. Similarly, follicles in BMB bulk gels remained in small clusters and exhibited low survival with only 1% of oocytes retrieved on day 18. In contrast, in the BMB fiber condition we observed cell contact with fibers, most probably via interactions with cell-deposited ECM and follicles survived and grew significantly better (Fig. 1c). Cell-ECM-fiber interactions enabled cell aggregation and fiber manipulation to form large multi-follicular structures within the hydrogels. Oocyte survival significantly improved compared to the control fiber and BMB bulk conditions with 14% live oocytes on day 18. Oocytes reached 43 μm in diameter, a significant increase compared to the control fiber condition. Immunohistochemical analysis for laminin, perlecan, and collagen I revealed significantly greater ECM deposition when cells were cultured with BMB-functionalized fibers compared to control fibers and bulk BMB hydrogels (Fig. 1d).

3.3. Cell-ECM but not cell-RGD interactions improve primordial follicle growth and survival

Next, we investigated differences in cell-matrix interactions via sequestered ECM compared to direct integrin binding to fibers functionalized with RGD (Fig. 2). Non-sequestering control hydrogels without DexVS fibers recapitulate the bulk mechanical stiffness of the ovarian ECM and allow proteolytic degradation, but without RGD or sequestered ECM present, have minimal cell-matrix interactions mediated by integrins. In this condition only 4.8% ± 0.6% of oocytes from

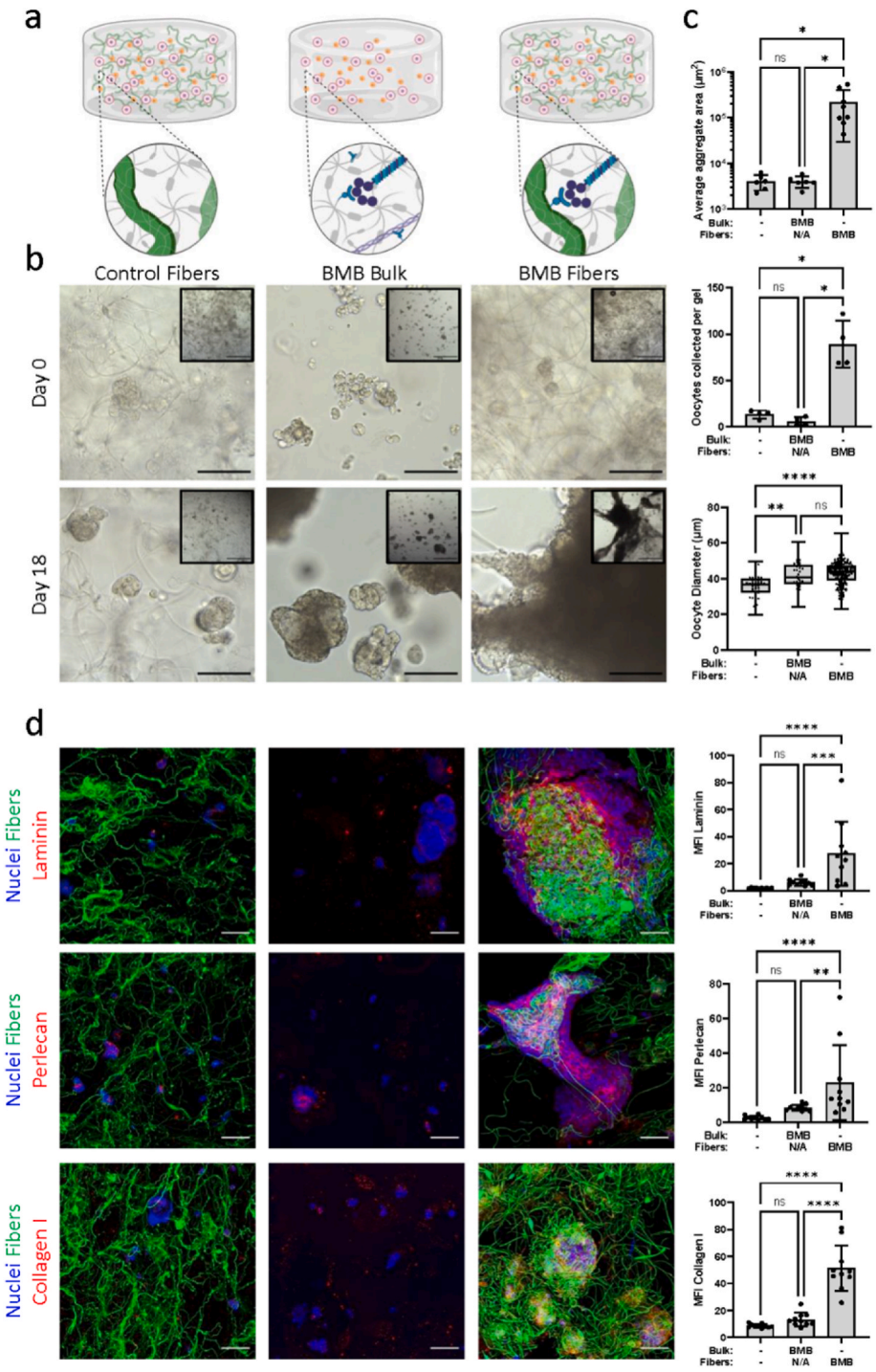

Fig. 1. Examining ECM deposition and cell aggregation via DexVS fibers and BMB peptide. (a) Schematics depicting culture conditions in non-sequestering bulk hydrogels embedded with non-sequestering DexVS fibers (control fibers), BMB-modified bulk hydrogels without DexVS fibers (BMB bulk), and non-sequestering bulk hydrogels with BMB-functionalized DexVS fibers (BMB fibers) in which BMB peptide will bind cell-secreted ECM proteins. Fibers were embedded in hydrogels at a 2% v/v density. (b) Representative brightfield images at 20× objective (scale bar 100 μm) and 5× objective (inset, scale bar 500 μm) after 0 and 18 days of culture. (c) Quantification of average aggregate cross-sectional area (−/− n = 6, BMB/NA n = 6, -/BMB n = 8), oocytes collected from each gel (n = 4 per condition), and oocyte diameters (oocytes pooled from 4 gels per condition, total oocytes: /- n = 53, BMB/NA n = 32, -/BMB n = 208) after 18 days of culture. (c) Representative confocal images of laminin, perlecan, and collagen type I (red) deposited by cells (nuclei, blue) in hydrogels with or without fibers (green) (scale bar 50 μm) with quantification of mean fluorescence intensity (MFI) of ECM normalized to nuclear stain (Hoechst) intensity (n = 10 samples per ECM per condition).

encapsulated follicles survived after 18 days of culture with an average oocyte diameter of 37.4 ± 5.7 μm. To test whether the lack of integrin-mediated interactions between cells and the gel was responsible for poor follicle survival, we incorporated DexVS fibers modified with RGD in non-sequestering PEG hydrogels (n = 9). In this condition we observed two different cellular organizations [1]: in 78% of the gels (7 of 9), follicles and cells aggregated in small clusters with minimal interactions with the RGD-fibers, and [2] in 22% of the gels (2 of 9), cells adhered to the RGD-fibers and formed a rather spread-out interconnected network of cells, which lost cell-oocyte connections and extruded the oocytes. A

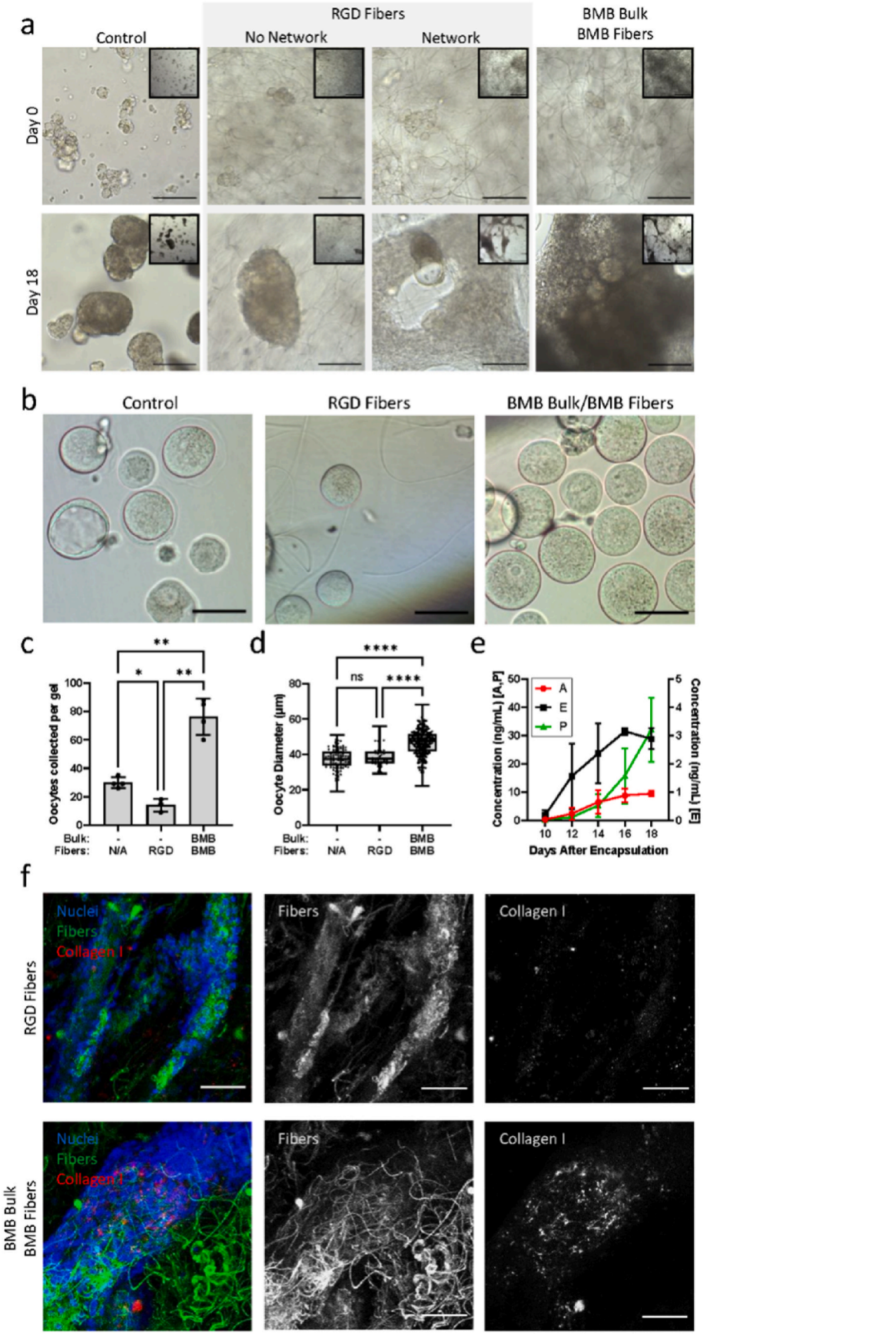

(caption on next page)

Fig. 2. ECM-sequestering peptides promoted ECM deposition and improved oocyte outcomes. (a) Representative brightfield images at 20× (scale bar 100 μm) and 5× objectives (inset, scale bar 500 μm) after 0 and 18 days of culture in unmodified PEG hydrogels (control), unmodified PEG gels embedded with 2%v/v RGD-functionalized DexVS fibers (RGD fibers), or BMB-modified PEG hydrogels embedded with 2%v/v BMB-functionalized DexVS fibers (BMB Bulk BMB Fibers). Cells cultured in hydrogels containing RGD fibers exhibited two distinct behaviors with 78% of hydrogels maintaining isolated cell clusters and 22% of hydrogels driving cell adhesion and network formation along fibers; (b) Representative images of oocytes collected from hydrogels after 18 days of culture. (c) Live oocytes collected from each gel (-/NA n = 4, -/RGD n = 3, BMB/BMB n = 4), and (d) oocyte diameter after 18 days of culture (-/NA n = 119 oocytes pooled from 4 gels, -/RGD n = 42 oocytes pooled from 3 gels, BMB/BMB n = 306 oocytes pooled from 4 gels). (e) Concentrations of steroid hormones androstenedione (A), estradiol (E), and progesterone (P) in medium collected from BMB Bulk/BMB Fiber hydrogels (n = 4). (f) Representative confocal images of collagen type I (red) deposition by cells (nuclei, blue) in hydrogels containing fibers (green) functionalized with either RGD or BMB (scale bar 50 μm).

macroscopic view of the hydrogels illustrates this distinct difference in cell behavior (Fig. 2a, Day 18 inset images). In both cases, oocyte survival and growth were poor, leading to only 2.3% ± 0.8% oocyte survival on day 18 and reaching 38.2 ± 5.3 μm in diameter. After confirming that RGD led to poor oocyte survival, we tested whether a different mechanism of cell-matrix interactions mediated by cell-deposited ECM would result in cell aggregation and follicle reorganization similar to native ovarian tissues. We incorporated BMB peptides in both DexVS fibers and the bulk of the PEG hydrogels to maximize sequestration of cell-secreted ECM. Follicles and cells cultured in this condition formed networks by pulling and incorporating the fibers in the clusters, forming more dense aggregates with BMB-fibers compared to RGD-fibers. Oocyte survival increased 2.5 and 5 times compared to non-sequestering and RGD-fibers controls reaching 12.4% ± 2.1% survival. The secretion of gonadal hormones from follicles cultured in the presence of BMB continuously increased, reaching 3 ng/mL of estradiol, 10 ng/mL of androstenedione and 30 ng/mL of progesterone, which is consistent with steroidogenic signatures of growing and maturing follicles (Fig. 2e). Continuously increasing hormone production is typical of follicles developing from the primordial to secondary and early antral stages [32]. High variance across samples is expected as each gel contains a large population of follicles at many different developmental stages. Analysis of cell-fiber and cell-matrix interactions revealed that in the RGD-fiber condition, cells adhered to fibers with minimal deposition of type I collagen in the tissue structures. In contrast, the deposition of type I collagen was significantly greater within the aggregates in the BMB-fiber condition (Fig. 2f). We concluded that while cells directly engaged with both RGD- and BMB-functionalized fibers, only the latter promoted follicle-localized ECM deposition and aggregation.

3.4. Density of ECM-sequestering fibers modulates cell aggregation

Having determined that BMB presentation on DexVS fibers leads to increased ECM deposition, cell aggregation, and improved oocyte survival, we sought to determine whether increasing the concentration of encapsulated fibers in the gel, i.e. fiber density (FD), would enable better connectivity between cells eventually contributing to contraction into larger aggregates. We encapsulated follicles in non-sequestering PEG embedded with BMB-functionalized fibers at varying densities to determine if oocyte survival and growth correlated with aggregate size (Fig. 3). Average aggregate size indeed increased with increasing fiber density, with an average cross-sectional area of approximately 18000 μm^2, 62000 μm^2, and 271000 μm^2 in the FD0.5%, FD1.0%, and FD2.0% conditions, respectively. Oocyte survival also increased with fiber density, with approximately 5.2%, 8.4%, and 15.8% oocyte survival in the FD0.5%, FD1.0%, and FD2.0% conditions, respectively. Importantly, oocytes that survived in all the conditions reached similar diameters of approximately 45 μm. Confocal analysis of deposited laminin, perlecan, and type I collagen revealed that these ECM components were present in aggregates of all sizes, suggesting that fibers presented balanced BMB sites for anchoring cell-secreted ECM.

Although fiber density has been shown to have negligible effects on bulk composite stiffness, the inclusion of synthetic fibers that are stiffer than the surrounding hydrogel may cause disparities in local mechanics and diffusion of soluble factors ([30], Supplemental Fig. 2). To control for effects that may arise from varying fiber density within the gels, we generated composites containing a fixed 2% v/v fraction of fibers but composed of different ratios of BMB-modified to control, cysteine-modified fibers (Fig. 4). Similar to our findings from experiments with increasing BMB-functionalized fiber density, cross-sectional area of aggregates increased with increasing proportions of BMB fibers, but no significant difference in oocyte survival or growth was observed. Upon visual inspection, it appeared more ECM is deposited in gels with greater proportions of BMB fibers, but when normalized to BMB-fiber content, no clear trends arise (Supplemental Fig. 3), suggesting that any amount of BMB present on fibers facilitates ECM sequestration and allows cells to aggregate.

3.5. Inhibition of hydrogel and ECM remodeling affect oocyte outcomes

Follicles were encapsulated in BMB-fiber embedded PEG hydrogels crosslinked by peptides possessing varying degrees of susceptibility to degradation to examine the effects of aggregate formation and proteolytic remodeling on oocyte survival and growth (Fig. 5). YKNR is a plasmin-sensitive sequence, naturally occurring in fibrin, whereas YKNS has a single amino acid substitution resulting in decreased enzyme affinity and slower rates of degradation. Hydrogels crosslinked with 100% YKNR degrade too fast and do not last until the end of culture [33]. On the contrary, hydrogels crosslinked with 100% YKNS degrade slower, but may be less permissive for cell proliferation [16,33]. Thus, mixing the two crosslinking peptides, YKNS and YKNR, enabled fine control of the speed of hydrogel degradation and resulted in the greatest follicle survival and growth [17]. Follicles encapsulated in hydrogels crosslinked with only YKNS with overall slower degradation formed smaller aggregates, but oocyte survival and growth matched that of the YKNS/YKNR hydrogels (Fig. 5b). Conversely, follicles cultured in hydrogels crosslinked with non-cleavable YK_DNS_D (D-YKNS) peptide did not interact with BMB fibers and oocyte survival and growth were significantly diminished. Marimastat, a broad-spectrum MMP-inhibitor, should only inhibit the degradation and remodeling of cell-deposited ECM and in theory should not directly affect plasmin-driven degradation of YKNS/YKNR crosslinked hydrogels. Marimastat-treated follicles did not form aggregates and oocyte survival was significantly decreased compared to control YKNS/YKNR crosslinked hydrogels where MMP activity was not inhibited. The few oocytes which survived grew to similar diameters as the degradable hydrogel conditions, but the yield was prohibitively low (less than 3%) for clinical translation. Immunofluorescent analysis revealed dense deposition of ECM in the YKNS/YKNR and YKNS only conditions, while very little ECM was observed in the presence of marimastat. Interestingly, collagen I was colocalized to BMB-fibers in the YK_DNS_D condition, but little laminin or perlecan was deposited (Supplemental Fig. 4).

4. Discussion

Synthetic hydrogels have long been used to mimic the bulk mechanical properties of tissue for organoid cultures, but organ architecture and function is dependent on complex microenvironmental cues not yet recapitulated by homogeneous hydrogels [34,35]. Recent advances in materials science now enable the creation of hierarchical composites with fibers surrounded by soft gel matrix, mimicking the composition of

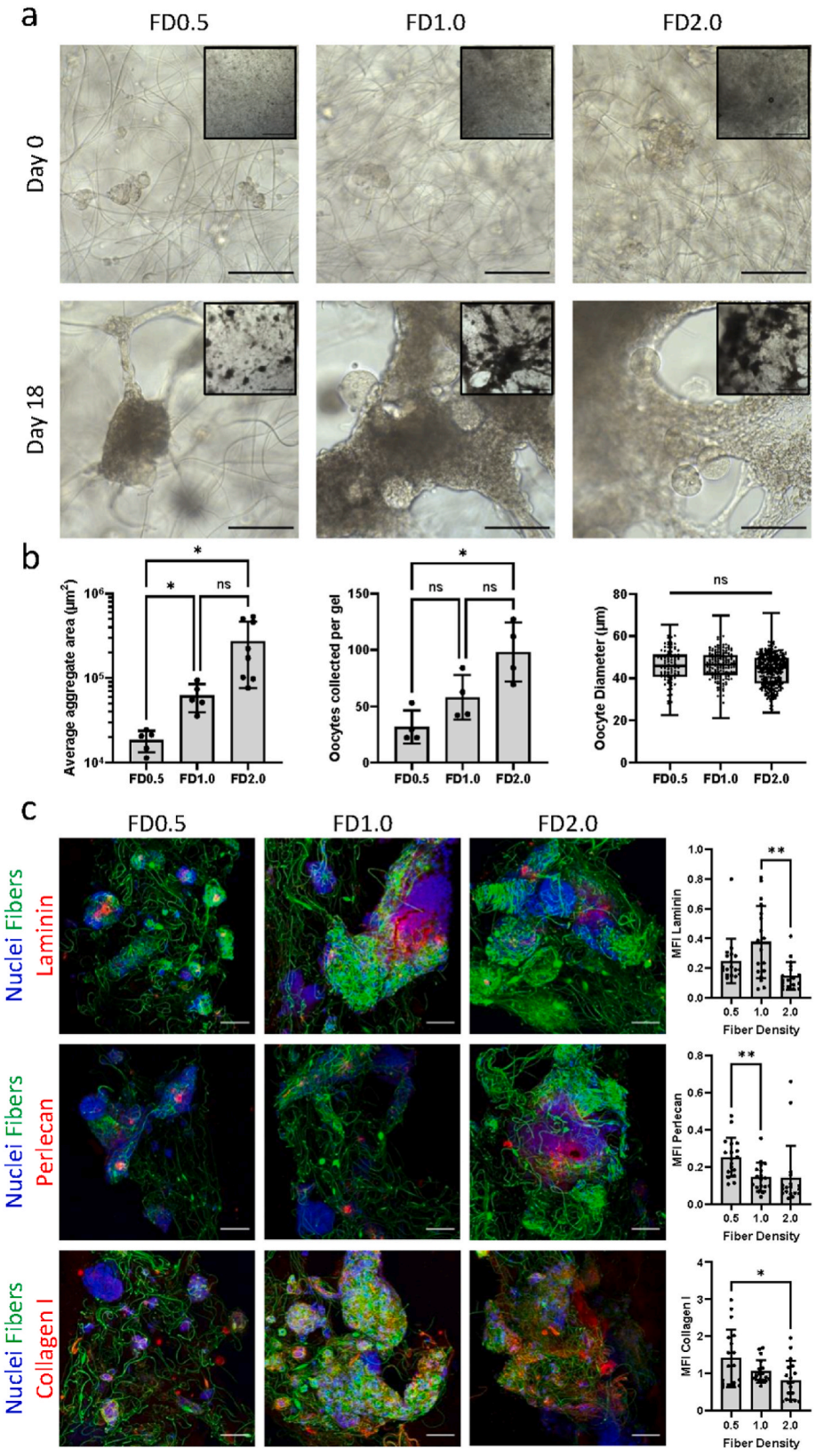

Fig. 3. Higher BMB fiber density in non-sequestering hydrogels increased aggregation and oocyte survival. (a) Representative brightfield images at 20× (scale bar 100 μm) and 5× objectives (inset, scale bar 500 μm) after 0 and 18 days of culture in gels of varying BMB-fiber density (FD, v/v%). (b) Quantification of average aggregate cross-sectional area (FD0.5 n = 5, FD1.0 n = 5, FD2.0 n = 8), oocytes collected from each gel (n = 4 per condition), and oocyte diameter after 18 days of culture (oocytes pooled from 4 gels per condition, total oocytes: FD0.5 n = 97, FD1.0 n = 169, FD2.0 n = 323). (c) Representative confocal images of laminin, perlecan, and collagen type I (red) in cell aggregates (nuclei, blue) formed around BMB-functionalized fibers (green) (scale bar 50 μm) with quantification of mean fluorescence intensity (MFI) of ECM normalized to nuclear stain (Hoechst) intensity (n = 18 samples per ECM per condition).

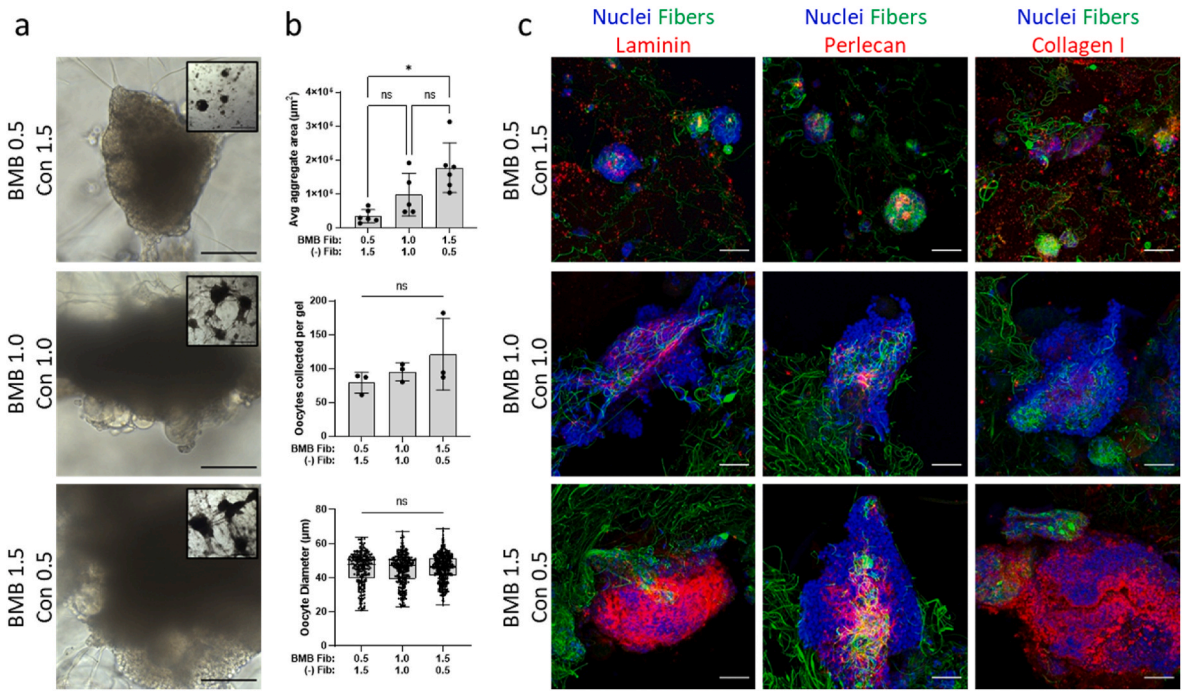

Fig. 4. Increased BMB proportion with constant fiber density did not affect oocyte outcomes. (a) Representative brightfield images of follicle and cell aggregates on Day 18 of culture at 20× (scale bar 100 μm) and 5× objectives (inset, scale bar 500 μm) when cultured in hydrogels of constant fiber density (2%v/v) with varied proportions of BMB-functionalized fibers (BMB) and unmodified fibers (Con). (b) Quantification of average aggregate cross-sectional area (0.5/1.5 n = 6, 1.0/1.0 n = 5, 1.5/0.5 n = 6), oocytes collected from each gel (n = 3 per condition), and oocyte diameter after 18 days of culture (oocytes pooled from 3 gels per condition, total oocytes: 0.5/1.5 n = 237, 1.0/1.0 n = 285, 1.5/0.5 n = 363). (c) Representative confocal images of laminin, perlecan, and collagen type I (red) in cell aggregates (nuclei, blue) formed around BMB-functionalized fibers (green) (scale bar 50 μm). Unmodified fibers are not fluorescently tagged in confocal images.

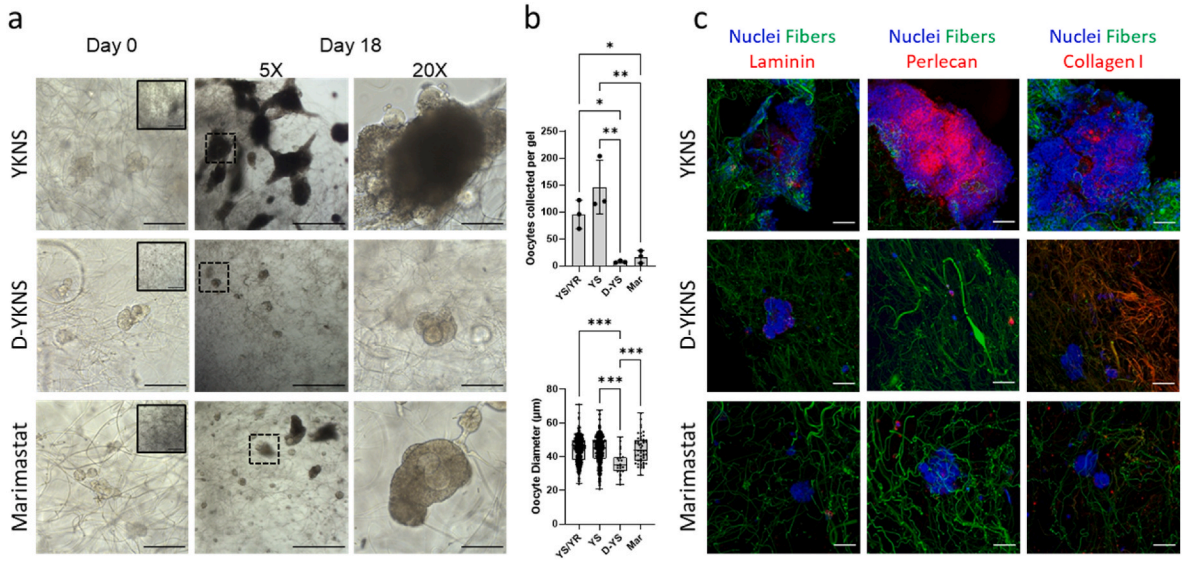

Fig. 5. Hydrogel degradability and ECM remodeling modulated cell interactions with BMB-functionalized fibers. All hydrogels embedded with 2%v/v BMB-functionalized fibers. (a) Representative brightfield images on Day 0 at 20× objective (5× objective, inset) and Day 18 of culture (20× scale bar 100 μm, 5× scale bar 500 μm). (b) Quantification of oocytes collected from each gel (n = 3 per condition), and oocyte diameter after 18 days of culture (oocytes pooled from 3 gels per condition, total oocytes: YS/YR n = 323, YS n = 439, D-YS n = 23, Mar n = 51). (c) Representative confocal images of laminin, perlecan, and collagen type I (red) deposited in follicle and cell aggregates (nuclei, blue) with BMB-functionalized fibers (green) (scale bar 50 μm). Abbreviations: hydrogels crosslinked with YKNS and YKNR (YS/YR), YKNS only (YS), nondegradable D-YKNS (D-YS), and YKNS/YKNR crosslinked hydrogels in which marimastat was added to the culture medium (Mar).

stromal ECM in native tissues [36]. Electrospun fibers, fabricated with varying stiffness, length, and diameters, model the diversity of fibrillar ECM components encountered *in vivo*, and functionalization of these fibers with bioactive peptides mimics the numerous biological functions of ECM. Here we employed ECM-binding peptides for sequestering cell-secreted proteins and proteoglycans on DexVS fibers within a PEG hydrogel and explored how peptide presentation and fiber density impacted ECM deposition and subsequent cell-matrix interactions

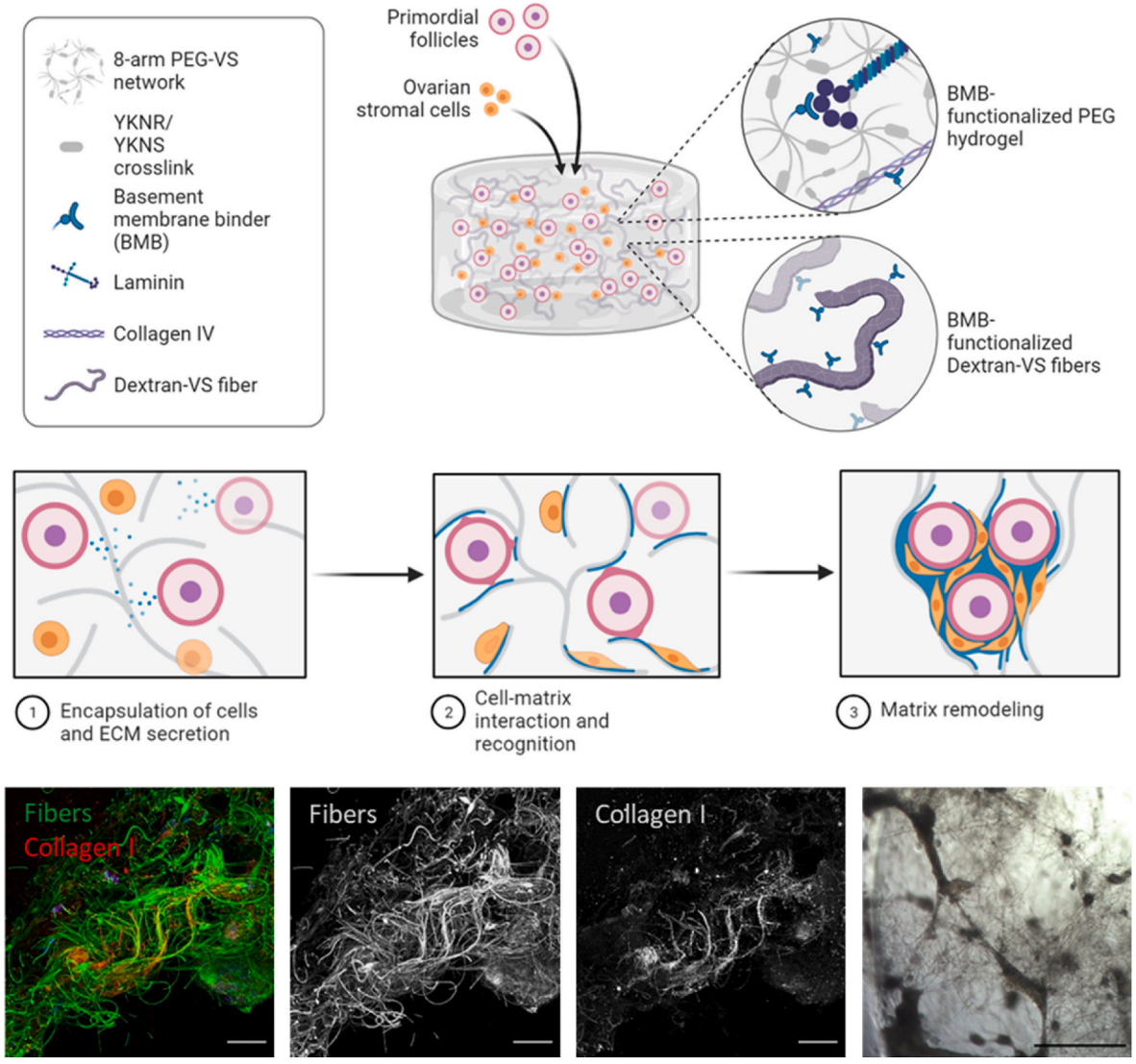

Fig. 6. Proposed mechanism of cell-secreted ECM sequestration and reorganization of the fibers. Schematic depicting follicle and cell encapsulation in degradable PEG hydrogels embedded with DexVS fibers and functionalized with ECM-sequestering BMB peptides. In the presence of BMB-functionalized Dextran-VS fibers, cell-secreted ECM, such as laminin and collagen, is sequestered along DexVS fibers, enabling cell adhesion and organization into tissue-like aggregates which restore critical cell-cell and cell-matrix interactions for improved oocyte survival and growth. Representative confocal and brightfield images depicting ECM alignment on fibers and cell aggregation facilitated by BMB-functionalized fibers (2% v/v in YKNS/YKNR crosslinked hydrogels).

(Fig. 6). To our knowledge, this is the first use of a fully synthetic hydrogel composite material to control the templating of cell-secreted ECM and allow aggregation and assembly of follicular organoid-like structures for a long-term culture.

Integrin binding sequences such as RGD have long been the gold standard to allow cells to bind to otherwise bioinert hydrogels, but these peptides are limited when compared to the range of interactions cells would have with the different components of native ECM. Conversely, BMB binds a multitude of cell-secreted ECM molecules, thereby creating layers of proteins and proteoglycans for cell-matrix interactions. Here we demonstrated that fiber functionalization with either RGD or BMB can promote cell adhesion, but only BMB conditions improved oocyte survival and growth compared to non-sequestering controls. We hypothesized that layering of multiple ECM components on BMB fibers diversifies and restores the cell-matrix interactions which were lost when follicles and cells were isolated from ovarian tissue for encapsulation. By sequestering cell-secreted ECM components, cell signaling pathways specific to ovarian ECM can be restored in the BMB conditions, as opposed to direct integrin interactions with RGD. Specifically, laminin and perlecan were deposited in BMB-functionalized conditions, both of which are present in follicle basement membranes and play important roles during folliculogenesis, such as steroid production and gonadotropin signaling [26,37,38]. Our previous study showed improved follicle growth and maturation with BMB and a laminin-derived peptide, AG73, likely because both sequences restored specific basement membrane interactions [17]. Here, we improved upon that system by using fibers as a scaffold for deposition and alignment, ultimately resulting in controlled ECM retention and templating within the hydrogels. This allowed ovarian follicles to reconstruct their native environment by depositing and remodeling matrix that preserved the delicate connections between cells through aggregation yet allowed growth and proliferation.

Throughout this study, we observed differences in oocyte growth and survival as a function of BMB peptide presentation, fiber density, and degradability of the bulk hydrogel. Importantly, the 3-fold increase in the yield of surviving oocytes has a tremendous clinical significance in improving the chances of obtaining a fertilizable egg. In general, conditions which contained BMB-functionalized fibers promoted cell

aggregation along with oocyte survival and growth. Conditions without BMB-fibers and conditions where interaction with BMB-fibers was inhibited, either physically in a non-degradable matrix or chemically through MMP inhibition, exhibited no aggregation and low oocyte survival. This indicates that critical cell-cell interactions are maintained within clusters, and ECM deposition on BMB-fibers facilitated aggregation into follicle-like structures, allowing immature follicles with minimal neighboring cells be pulled into clusters and rescued, overall promoting the survival of encapsulated follicles. Our findings further suggest that the aggregates formed with the fibers do not collapse or densify over time, supporting the notion of reciprocal remodeling, e.g., degradation and deposition of new ECM.

The presence of BMB-functionalized fibers allowed cells and follicles to aggregate, which was critical for oocyte survival; however, the size of the aggregates did not correlate with the oocyte survival. It is likely that the key cell-cell interactions restored upon initial aggregation in both conditions were sufficient to support oocyte survival. Decoupling the relationship between aggregate size and oocyte survival was more complicated when considering fiber density. Hydrogels with increasing fiber density exhibited both increased oocyte survival and aggregate size, which we attributed to higher probability of cells to interact with fibers at higher densities. However, when controlling for total fiber density within in the hydrogel with varying BMB modification, aggregate sizes increased with BMB-functionalized fiber proportions while oocyte survival was unaffected. We hypothesized that BMB-functionalized fibers served as initiators for aggregation and unmodified fibers entangled within BMB-fibers may pull additional cells and follicles into the aggregate as cells remodel ECM bound to the BMB-fibers. In doing so, follicles and cells can form small, localized aggregates that improve oocyte survival even at low BMB-fiber proportions. Across these conditions, it is evident that the formation of aggregates significantly improves oocyte survival and growth, however the size of the aggregate may be negligible. While the precise mechanisms are still to be elucidated, we hypothesize that aggregates bring together a diverse range of cell types, any of which may provide key signals for oocyte development, and the cellular composition of the aggregates will need to be further studied to understand which populations are providing key support for folliculogensis.

5. Conclusion

In summary, we have developed an ECM-sequestering matrix for primordial follicle culture and have shown improved oocyte survival and growth when follicles and cells are encapsulated in degradable PEG hydrogels embedded with electrospun DexVS fibers functionalized with ECM-sequestering peptide, BMB, to serve as a scaffold for ECM deposition and remodeling, replicating the fibrous structure of native ECM. ECM deposition on fibers not only restores direct cell-matrix interactions which improve oocyte growth, but also facilitates cell aggregation to restore cell-cell interactions for oocyte survival (Fig. 6). By facilitating ECM deposition and cell aggregation in a degradable hydrogel, we were able to mimic the physical and chemical cues present in the native ovary. The biomimetic hydrogel presented here is a promising platform for *in vitro* follicle culture and a potential fertility preservation option for women undergoing gonadotoxic cancer therapies. Further studies could employ this culture system to decipher the precise mechanisms of cell-cell and cell-matrix binding in an artificial ovary, explore key regulators of early stage folliculogenesis, identify essential ovarian stromal cell populations for follicle support, and could also be applied to the broader field of tissue engineering.

CRediT authorship contribution statement

Claire E. Nason-Tomaszewski: Conceptualization, Methodology, Investigation, Visualization, Formal analysis, Project administration, Writing, editing and revision. **Emily E. Thomas:** Methodology, Investigation, Visualization, Formal analysis, Formal analysis, Project administration, Writing, editing and revision. **Daniel L. Matera:** Methodology, Methodology, Investigation, Visualization, Formal analysis, Project administration, Writing, editing and revision. **Brendon M. Baker:** Conceptualization, Methodology, Investigation, Visualization, Formal analysis, Project administration, Supervision, Funding acquisition, Writing, editing and revision. **Ariella Shikanov:** Conceptualization, Methodology, Investigation, Visualization, Formal analysis, Project administration, Supervision, Funding acquisition, Writing, editing and revision.

Declaration of competing interest

The authors declare that they have no known competing financial interests or personal relationships that could have appeared to influence the work reported in this paper.

Acknowledgements

The authors would like to acknowledge the University of Virginia Center for Research in Reproduction Ligand Assay and Analysis Core (Eunice Kennedy Shriver NICHD/NIH Grant R24HD102061) for performing the hormone assays. This work was supported by the National Institutes of Health (R01 HD099402 to AS, R01 EB030474 to BMB, F31 HD100069 to CENT) and the Juvenile Diabetes Research Foundation (1-INO-2020-916-A-N to BMB). This material is based upon work supported by the National Science Foundation Graduate Research Fellowship Program under Grant No. DGE 1841052. DLM acknowledges funding from the Rackham Graduate School Predoctoral fellowship. All schematics were created using BioRender.com.

Appendix A. Supplementary data

Supplementary data to this article can be found online at https://doi.org/10.1016/j.bioactmat.2023.10.001.

References

[1] C. Bonnans, J. Chou, Z. Werb, Remodelling the extracellular matrix in development and disease, Nat. Rev. Mol. Cell Biol. 15 (2014).
[2] A.D. Theocharis, S.S. Skandalis, C. Gialeli, N.K. Karamanos, Extracellular Matrix Structure, vol. 97, Advanced Drug Delivery Reviews, 2016.
[3] M.W. Tibbitt, K.S. Anseth, Hydrogels as extracellular matrix mimics for 3D cell culture, Biotechnol. Bioeng. 103 (2009).
[4] M. Hofer, M.P. Lutolf, Engineering organoids, Nat. Rev. Mater. 6 (2021).
[5] C. Gutierrez, J. Ralph, E. Telfer, I. Wilmut, R. Webb, Growth and antrum formation of bovine preantral follicles in long-term culture in vitro, Biol Reprod. Biol Reprod. 62 (5) (2000) 1322–1328.
[6] H.M. Picton, S.E. Harris, W. Muruvi, E.L. Chambers, The in vitro growth and maturation of follicles, Reproduction 136 (6) (2008) 703–715.
[7] Y. Zhang, Z. Yan, Q. Qin, V. Nisenblat, H.M. Chang, Y. Yu, et al., Transcriptome landscape of human folliculogenesis reveals oocyte and granulosa cell interactions, Mol. Cell 72 (6) (2018) 1021–1034.e4.
[8] M. Binelli, B.D. Murphy, Coordinated regulation of follicle development by germ and somatic cells, Reprod. Fertil. Dev. 22 (1) (2010) 1–12.
[9] A. Converse, E.J. Zaniker, F. Amargant, F.E. Duncan, Recapitulating folliculogenesis and oogenesis outside the body: encapsulated in vitro follicle growth, Biol. Reprod. 108 (1) (2023) 5–22.
[10] A.J.W. Hsueh, K. Kawamura, Y. Cheng, B.C.J.M. Fauser, Intraovarian control of early folliculogenesis, Endocr. Rev. 36 (1) (2015) 1–24.
[11] J.E. Hornick, F.E. Duncan, L.D. Shea, T.K. Woodruff, Multiple follicle culture supports primary follicle growth through paracrine-acting signals, Reproduction 145 (1) (2013) 19–32.
[12] H. Zhou, J.T. Decker, M.M. Lemke, C.E. Tomaszweski, L.O.D. Hea, K.B. Arnold, et al., Synergy of Paracrine Signaling during Early-Stage Mouse Ovarian Follicle Development in Vitro, 2018.
[13] A. Jones, B.P. Bernabé, V. Padmanabhan, J. Li, A. Shikanov, Capitalizing on transcriptome profiling to optimize and identify targets for promoting early murine folliculogenesis in vitro, Sci. Rep. 11 (1) (2021).
[14] C.M. Tingen, S.E. Kiesewetter, J. Jozefik, C. Thomas, D. Tagler, L. Shea, et al., A macrophage and theca cell-enriched stromal cell population influences growth and survival of immature murine follicles in vitro, Reproduction 141 (6) (2011) 809–820.

[15] D. Tagler, T. Tu, R.M. Smith, N.R. Anderson, C.M. Tingen, T.K. Woodruff, et al., Embryonic fibroblasts enable the culture of primary ovarian follicles within alginate hydrogels, Tissue Eng. Part A [Internet 18 (11–12) (2012), 1229–38. Available from: http://online.liebertpub.com/doi/abs/10.1089/ten.tea.2011.0418 .
[16] C.E. Tomaszewski, E. Constance, M.M. Lemke, H. Zhou, V. Padmanabhan, K. B. Arnold, et al., Adipose-derived stem cell-secreted factors promote early stage follicle development in a biomimetic matrix, Biomater. Sci. 7 (2) (2019) 571–580.
[17] C.E. Tomaszewski, K.M. DiLillo, B.M. Baker, K.B. Arnold, A. Shikanov, Sequestered cell-secreted extracellular matrix proteins improve murine folliculogenesis and oocyte maturation for fertility preservation, Acta Biomater. (2021) 132.
[18] C.B. Berkholtz, L.D. Shea, T.K. Woodruff, Extracellular matrix functions in follicle maturation, Semin. Reprod. Med. 24 (4) (2006), 262-9.
[19] S. Joo, S.H. Oh, S. Sittadjody, E.C. Opara, J.D. Jackson, S.J. Lee, et al., The effect of collagen hydrogel on 3D culture of ovarian follicles, Biomed. Mater. 11 (6) (2016).
[20] T.E. Curry, K.G. Osteen, The matrix metalloproteinase system: changes, regulation, and impact throughout the ovarian and uterine reproductive cycle, Endocr. Rev. 24 (2003).
[21] S. Jordahl, L. Solorio, D.B. Neale, S. McDermott, J.H. Jordahl, A. Fox, et al., Engineered fibrillar fibronectin networks as three-dimensional tissue scaffolds, Adv. Mater. 31 (46) (2019) 1–10.
[22] C. Loebel, R.L. Mauck, J.A. Burdick, Local nascent protein deposition and remodelling guide mesenchymal stromal cell mechanosensing and fate in three-dimensional hydrogels, Nat. Mater. 18 (8) (2019).
[23] A. Shikanov, M. Xu, T.K. Woodruff, L.D. Shea, Interpenetrating fibrin-alginate matrices for in vitro ovarian follicle development, Biomaterials [Internet] 30 (29) (2009) 5476–5485, https://doi.org/10.1016/j.biomaterials.2009.06.054.
[24] J. Lam, N.F. Truong, T. Segura, Design of cell-matrix interactions in hyaluronic acid hydrogel scaffolds, Acta Biomater [Internet] 10 (4) (2014) 1571–1580, https://doi.org/10.1016/j.actbio.2013.07.025.
[25] A.M. Rosales, S.L. Vega, F.W. DelRio, J.A. Burdick, K.S. Anseth, Hydrogels with reversible mechanics to probe dynamic cell microenvironments, Angew. Chem., Int. Ed. 56 (40) (2017) 12132–12136.
[26] J. Grosbois, E.C. Bailie, T.W. Kelsey, R.A. Anderson, E.E. Telfer, Spatio-temporal remodelling of the composition and architecture of the human ovarian cortical extracellular matrix during in vitro culture, Hum. Reprod. 38 (3) (2023) 444–458.
[27] T.I.R. Hopkins, V.L. Bemmer, S. Franks, C. Dunlop, K. Hardy, I.E. Dunlop, Micromechanical mapping of the intact ovary interior reveals contrasting mechanical roles for follicles and stroma, Biomaterials 277 (2021).
[28] C.D. Wood, M. Vijayvergia, F.H. Miller, T. Carroll, C. Fasanati, L.D. Shea, et al., Multi-modal magnetic resonance elastography for noninvasive assessment of ovarian tissue rigidity in vivo, Acta Biomater. 13 (2015).
[29] E. Ouni, A. Peaucelle, K.T. Haas, O. Van Kerk, M.M. Dolmans, T. Tuuri, et al., A blueprint of the topology and mechanics of the human ovary for next-generation bioengineering and diagnosis, Nat. Commun. 12 (1) (2021).
[30] D.L. Matera, W.Y. Wang, M.R. Smith, A. Shikanov, B.M. Baker, Fiber density modulates cell spreading in 3D interstitial matrix mimetics, ACS Biomater. Sci. Eng. 5 (6) (2019).
[31] Q.P. Pham, U. Sharma, A.G. Mikos, Electrospinning of Polymeric Nanofibers for Tissue Engineering Applications: A Review, vol. 12, Tissue Engineering, 2006.
[32] J. Zhang, B.A. Goods, P. Pattarawat, Y. Wang, T. Haining, Q. Zhang, et al., An ex vivo ovulation system enables the discovery of novel ovulatory pathways and nonhormonal contraceptive candidates, Biol. Reprod. 108 (January) (2023) 629–644.
[33] A. Shikanov, R.M. Smith, M. Xu, T.K. Woodruff, L.D. Shea, Hydrogel network design using multifunctional macromers to coordinate tissue maturation in ovarian follicle culture, Biomaterials 32 (10) (2011) 2524–2531.
[34] N. Gjorevski, M. Nikolaev, T.E. Brown, O. Mitrofanova, N. Brandenberg, F. W. DelRio, et al., Tissue geometry drives deterministic organoid patterning, Science (6576) (2022) 375.
[35] J. Kim, B.K. Koo, J.A. Knoblich, Human organoids: model systems for human biology and medicine, Nat. Rev. Mol. Cell Biol. 21 (2020).
[36] J.M. Shapiro, M.L. Oyen, Hydrogel composite materials for tissue engineering scaffolds, JOM 65 (4) (2013).
[37] M.E. McArthur, H.F. Irving-Rodgers, S. Byers, R.J. Rodgers, Identification and immunolocalization of decorin, versican, perlecan, nidogen, and chondroitin sulfate proteoglycans in bovine small-antral ovarian follicles, Biol. Reprod. 63 (3) (2000).
[38] A. Logan, D.J. Hill, Bioavailability: is this a key event in regulating the actions of peptide growth factors? Vol. 134, J. Endocrinol. 134 (2) (1992), 157-61.